Ore Geology Reviews 73 (2016) 346–353

Contents lists available at ScienceDirect

Ore Geology Reviews

journal homepage: www.elsevier.com/locate/oregeorev

A fluid inclusion study of the Hetai goldfield in the Qinzhou Bay–Hangzhou Bay metallogenic belt, South China

Yi Zheng [a,b,*], Yongzhang Zhou [b,*], Yuejun Wang [b], Wenjie Shen [a], Zhijun Yang [a], Xingyuan Li [a], Fan Xiao [a]

[a] School of Earth Sciences and Geological Engineering, Sun Yat-sen University, Guangzhou 510275, China
[b] Guangdong Provincial Key Lab of Geological Processes and Mineral Resource Survey, Guangzhou 510275, China

ARTICLE INFO

Article history:
Received 18 May 2014
Received in revised form 7 September 2014
Accepted 9 September 2014
Available online 16 September 2014

Keywords:
Hetai goldfield
Fluid inclusions (FIs)
Ductile shear zones
Orogenic gold deposits
South China

ABSTRACT

The Hetai goldfield is located in the southern section of the Qinzhou Bay–Hangzhou Bay metallogenic belt (QHMB), South China. Gold mineralization is controlled by NE-trending ductile shear zones. Gold grade is higher at the shear zone centers and decreases sharply away from the shear zones, regardless of the host rock type. Fluid inclusions (FIs) preserved in the auriferous quartz veins have been analyzed to constrain their genesis. Three types of gold mineralization-related FIs, including moderate-salinity aqueous (A-type), low-salinity H_2O–CO_2 (B-type) and CO_2-dominated (C-type), have been newly identified. The measured homogenization temperatures (T_h) range from 130 °C to 310 °C, with two peaks of about 245 °C and 170 °C. The calculated pressures of FIs range from 50 MPa to 170 MPa. Immiscibility and CO_2 effervescence of fluids may have played an important role in gold precipitation during the ascent of the ore-forming fluids. The Hetai goldfield is a typical example of orogenic gold deposits originating from auriferous metamorphic fluids.

1. Introduction

Orogenic gold deposits occur as fault-controlled lodes in the greenschist facies metamorphic terranes formed in accretionary or collisional orogens (Groves et al., 1998). A number of characteristics were used to identify orogenic gold deposits, viz.: 1) Orogenic gold deposits are formed in convergent, collisional to post-collisional tectonic settings (Chen, 2006; Chen and Fu, 1992); 2) the location and occurrence of orebodies are controlled by brittle to ductile structures (Kerrich et al., 2000); 3) the host rock lithologies vary, and are commonly metamorphosed from lower- to upper greenschist facies, and less commonly to lower amphibolite facies (Goldfarb et al., 2001); 4) alteration mineral assemblages are dominated by carbonate − sulfide ± sericite ± chlorite (Groves et al., 2003; Li et al., 2012); 5) element associations include Au, Ag, As, Sb, Hg, W, Mo, Te and B (Reich et al., 2005; Zhang et al., 2014); 6) the ore-forming process is characterized by mesothermal, low salinity, and carbon-rich fluids originating from metamorphic devolatilization (Chen et al., 2007; Phillips and Powell, 2010; Zhang et al., 2012). These characteristics have facilitated the recognition of some orogenic gold deposits, such as those in the Yilgarn Craton and Bendigo goldfields in Australia (Hagemann and Luders, 2003; Thomas et al., 2011), the Donlin Creek gold deposit (Alaska) in North America (Goldfarb et al., 2004), the giant Sukhoi Log gold deposit (Siberia) in Russia (Large et al., 2007, 2009), as well as in Qinling (i.e., Henan, Shaanxi and Gansu provinces), Jiaodong (Shandong Province) and Xinjiang Province in China (Chen et al., 2001, 2012a, 2012b; Fan et al., 2003; Li et al., 2008, 2011; Nie, 1997; Zhou et al., 2002).

The Qinzhou Bay–Hangzhou Bay metallogenic belt (QHMB) is one of the most important metallogenic belts in South China. The QHMB is associated with the Qinzhou Bay–Hangzhou Bay Juncture Orogenic Belt, which has been interpreted as a giant tectonic suture between the Yangtze and Cathaysia blocks that has experienced multi-stage orogeny from the Neoproterozoic to the Mesozoic (Pirajno and Bagas, 2002; Shu et al., 2011; Wang et al., 2003, 2008, 2013; Zhao and Cawood, 2012; Zhou et al., 2012). The suture is about 2000 km long and 70–130 km wide, extending from the Qinzhou Bay in Guangxi, through northwestern Guangdong, eastern Hunan and middle Jiangxi, to Hangzhou Bay in Zhejiang (Fig. 1). The southern section of the QHMB is one of the most important gold-producing areas in China (Wang et al., 1997; Zhou et al., 2012). Compared with the Jiaodong and Qinling gold deposit clusters (Fan et al., 2003; Li et al., 2008, 2011), gold deposits in the southern QHMB are less well documented in the international literature (Chen and Wang, 1994; Pirajno and Bagas, 2002; Zhang et al., 2001). The Hetai goldfield is located in the southern QHMB (Fig. 1), with proven gold reserves of over 100 t grading at 7 g/t, e.g., the Gaocun and Yunxi gold deposits contain 21 t and 18 t gold, respectively (Wang and Yao, 2001). The ore-forming fluids have been argued to be magmatic hydrothermal, metamorphic, meteoric or their mixing products (Li et al., 2001; Liu et al., 2005; Wang et al., 1997; Zhou, 1992). More specific studies on compositions and source of the fluids were needed to

* Corresponding authors at: No. 135 West Xingang Road, Haizhu District, Guangzhou 510472, China. Tel.: +86 20 84110735.
E-mail addresses: zhengy43@mail.sysu.edu.cn (Y. Zheng), zhouyz@mail.sysu.edu.cn (Y. Zhou).

http://dx.doi.org/10.1016/j.oregeorev.2014.09.008
0169-1368/

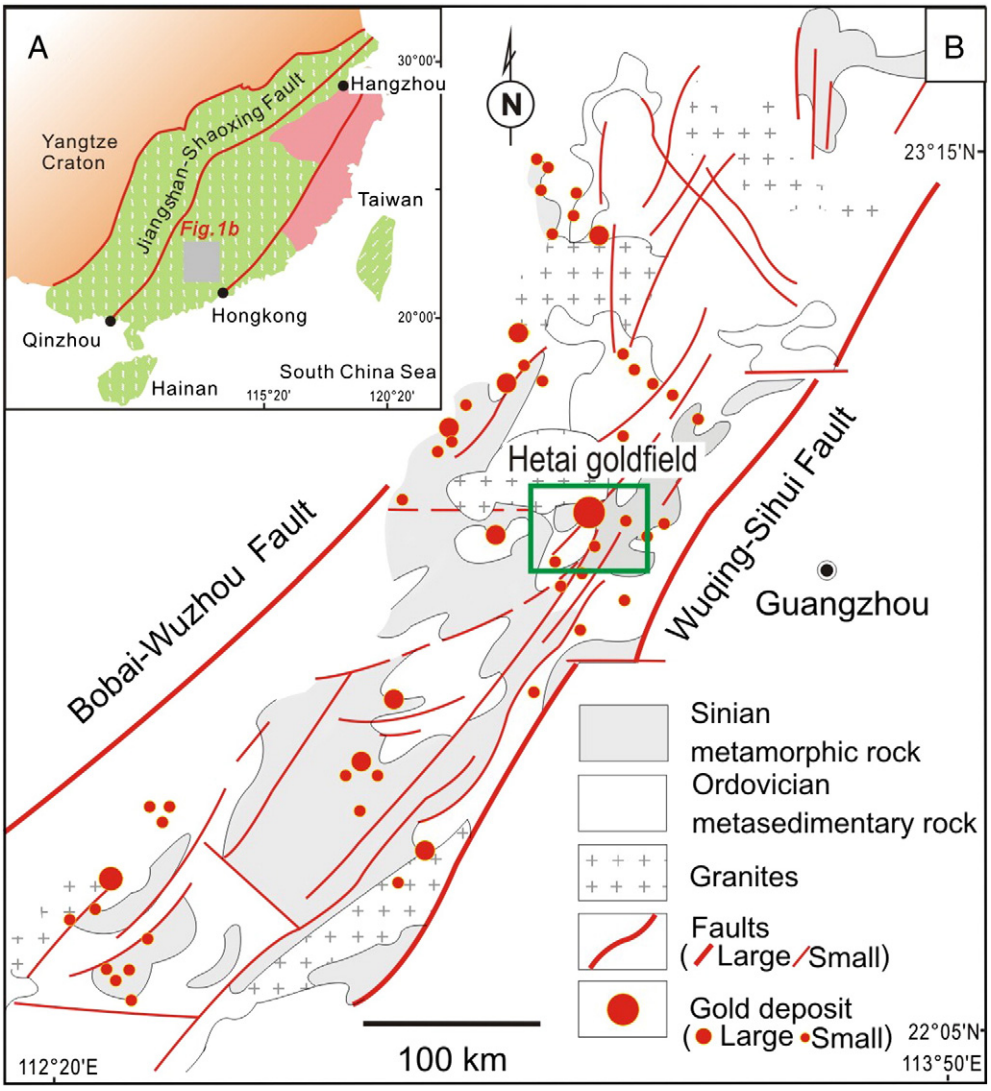

Fig. 1. Tectonic outline and distribution of gold deposits in the western Guangdong Province, South China.

enhance our knowledge on this giant gold field and to provide guidance for future exploration in this region.

The formation of gold deposits normally occurs as a consequence of various geological and geochemical conditions that are important to ore deposit model. Among the many contributing factors, the hydrothermal fluid is critical on the significant amount of gold (Chen et al., 2007; Lu et al., 2004; Pirajno, 2009). Changes in physiochemical conditions of the hydrothermal fluids and their interactions with the wall rocks have often led to the precipitation of gold from the solution (Li et al., 2012). Thus, the nature and compositions of hydrothermal fluids in the formation of gold deposit are becoming an increasingly important topic of research (Chen et al., 2007).

This contribution focuses on the fluid inclusions (FIs) preserved in the auriferous quartz veins of the Hetai goldfield. We will unravel the geochemical characteristics of these FIs and their metallogenic implications, with the aim to provide a case study to guide investigation of similar types of gold deposits in South China.

2. Geological background

The Hetai goldfield is situated in the western Guangdong Province, part of the southern section of the QHMB (Fig. 1). The gold deposits exposed in the mineral field include Xiniuding, Taipingding, Shangtai, Yunxi, Taozishan, Kangwei, Gaocun, Huojing and Hehai (Fig. 2).

It has been suggested that these gold deposits belong to the altered ductile shear zone-hosted type (Pirajno and Bagas, 2002; Wang et al., 1997; Zhou et al., 1995). The altered ductile shear zones are the most critical parameters for the formation of gold deposits. The NE-trending ductile shear zones control the geometry, extent and occurrence of the gold orebodies (Fig. 2). Gold abundance increases from anomalous level to a peak wherever a deformation zone is encountered, regardless of the host rock lithologies, and decreases sharply away from the shear zones.

The rock units exposed in the Hetai mining area are predominantly Sinian metamorphic rocks and Ordovician metasedimentary rocks (Fig. 2). The thick Sinian strata, subjected to migmatization and intruded by granodiorite (197 to 233 Ma, Wang et al., 1997), are the most important host rocks for the gold deposits, and they have been interpreted to have originated from terrigenous marine flysch sedimentary rocks intercalated with bedded cherts (No. 719 Geol. Team, 1987; Zhou, 1992; Zhou et al., 1994a). The migmatites at Hetai contain mainly plagioclase and quartz and minor biotite (Fig. 3A), whereas the Sinian schists contain mainly sericite and quartz (Fig. 3B).

The gold orebodies in the mining area are mainly controlled by a Hercyno-Indosinian deformation system comprising numerous NE-trending ductile shear zones (Fig. 2; Pirajno and Bagas, 2002; Wang et al., 1997). In the shear zones, deformation gradually increases inward towards the deformation center, with the rocks changing from

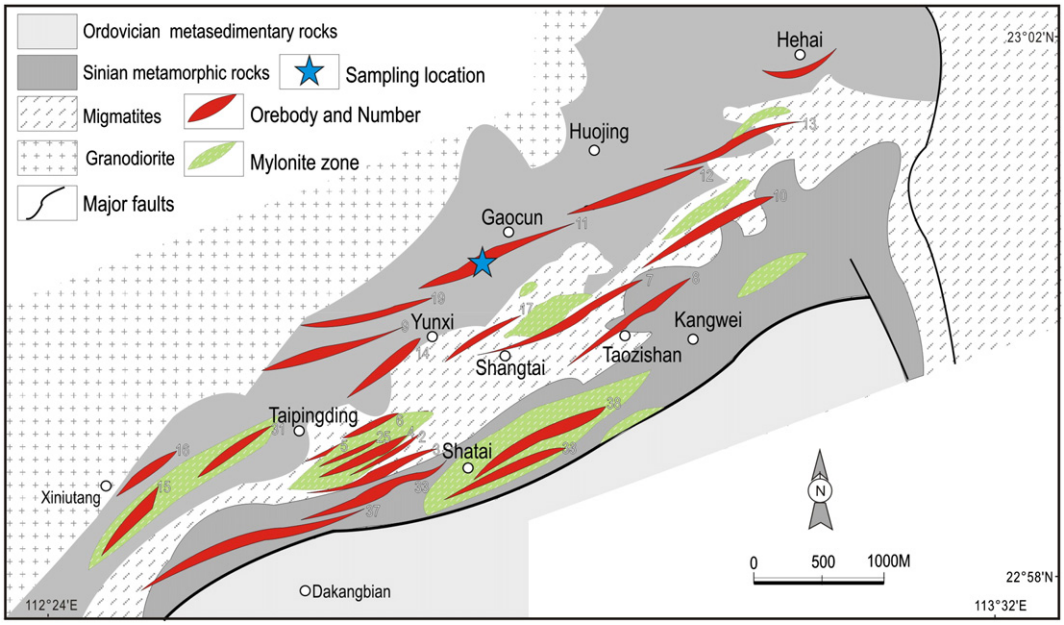

Fig. 2. Distribution of the mylonite zones and gold deposits in the Hetai goldfield, South China. Modified after the No. 719 Geological Team (1987).

undeformed protoliths, through proto-mylonite to mylonite. Three sets of planar fabrics, namely S, C and E, and typical deformation textures are observed. The characteristic deformation pattern comprises domains of anatomizing shear fabrics separating rhomboid domains of less deformed rocks (Fig. 2; Zhou et al., 1994b).

Wall-rock hydrothermal alteration is both spatially and temporally associated with the development of the ductile shear system (Fig. 2). The alteration products include hydrothermal quartz, sulfides, muscovite and ankerite (Chen and Wang, 1994; Zhang et al., 2001). Silicic alteration occurred throughout the alteration processes. There are two groups of auriferous quartz: 1) early lenticular quartz veins are associated with large amount of sulfide and higher-grade gold; and 2) late auriferous veins cross-cut the earlier lenticular quartz veins and contain fewer sulfide and lower-grade gold (Fig. 3C and D). Additionally, the altered mylonites also contain minor gold with important economic value. The minerals of economic importance disseminated in the ores and host-

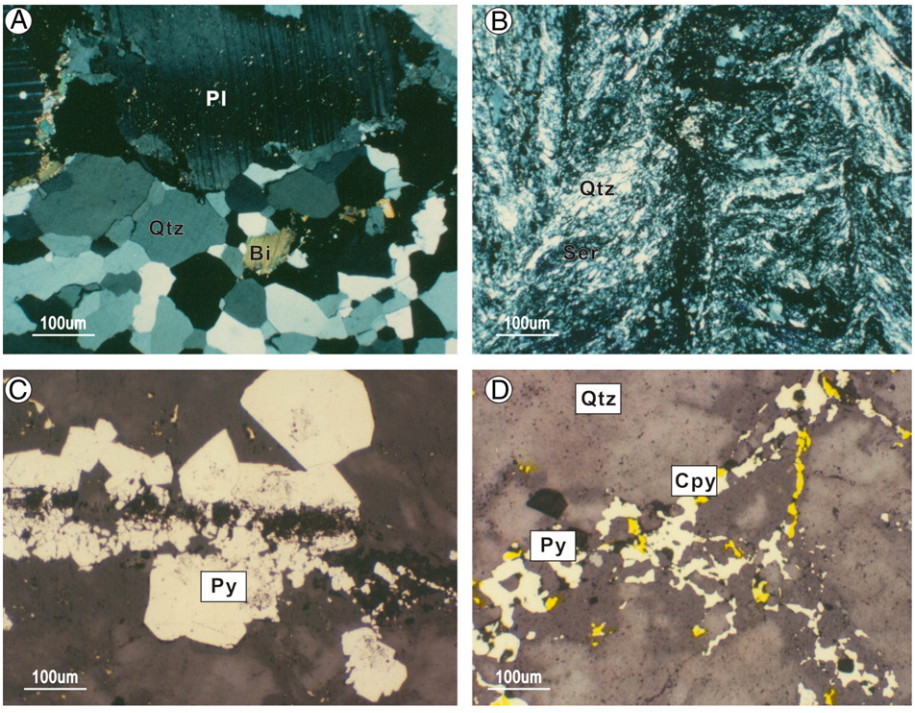

Fig. 3. Microphotographs illustrating the alterations of the host rocks and ores at Hetai. (A) The migmatites consisting of quartz (Qtz), plagioclase (Pl) and biotite (Bi); (B) the schists consisting of quartz (Qtz) and sericite (Ser); (C) pyrite (Py) occurring in the gold-bearing quartz veins; (D) pyrite (Py) and chalcopyrite (Cpy) occurring in the gold-bearing quartz veins.

rocks include native gold, chalcopyrite and pyrite (Fig. 3C and D). Gold precipitation is closely related to the formation of hydrothermal quartz and sulfides (Fig. 4A and B; Zhou, 1992).

3. Fluid inclusion characteristics

3.1. Sampling and analytical methodology

20 samples of the auriferous sulfide-bearing quartz veins were selected for FI analyses. Microthermometric measurements on FIs were performed using a Linkam THMS MDS600 heating–freezing stage (from −196 °C to 550 °C) at the Sun Yat-sen University. The precision of temperature measurements is approximately ±0.1 °C on cooling runs and ±2 °C on heating runs. The heating/freezing rate was generally 0.2–5 °C/min, but reduced to less than 0.2 °C/min near phase transformation. Salinities of aqueous FIs were estimated using the reference data of Bodnar (1993) for the NaCl–H_2O system. Salinities of CO_2-bearing FIs were calculated using the equations of Collins (1979). Densities were calculated using the FLINCOR software according to the microthermometry data of Brown and Lamb (1989).

3.2. FI classification

There are no significant differences in the FI content and type for the two auriferous quartz vein types. Three major FI types, namely A-, B- and C-types, were identified based on the phases occurring at room temperature and their behavior under heating and cooling. The slight difference is that the early lenticular veins contain more pseudosecondary FIs along the oriented healed fractures, whereas the late hydrothermal veins contain more isolated primary FIs.

3.2.1. A-type FIs

This FI type commonly contains a liquid and a vapor phase at room temperature (Fig. 4C). Both phases are aqueous, which are confirmed by subsequent microthermometry data. Daughter minerals have not been detected in the FIs of this type.

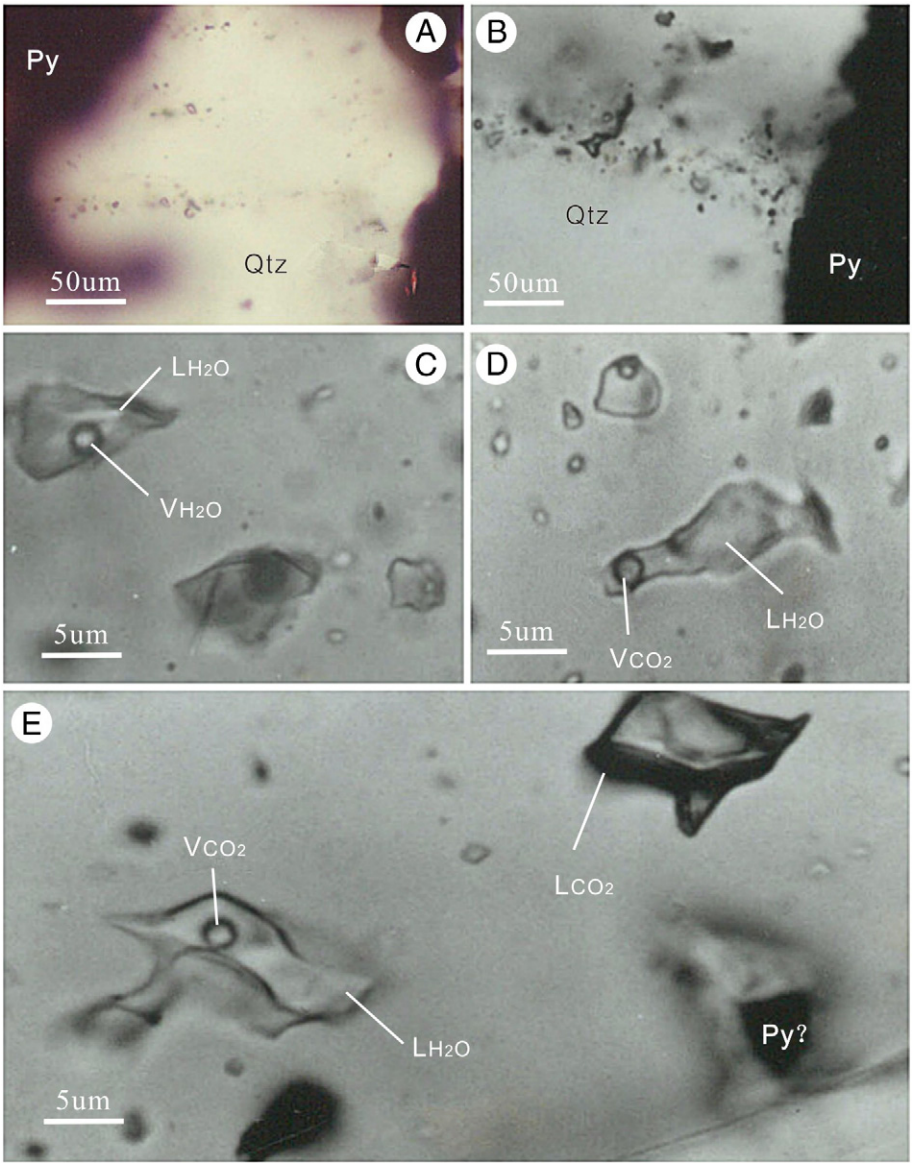

Fig. 4. Occurrence of FIs in host quartz grains from the Hetai goldfield, southern China. (A) Oriented distribution of FIs along healed fractures, as indicated by trail of FIs. (B) Trail of FIs "cuts" through host quartz, but ends abruptly at the contacts between quartz and sulfides. The opaque mineral is pyrite (Py), and the pale white mineral is quartz (Qz); (C) moderate-salinity aqueous inclusions (A-type FIs); (D) low-salinity H_2O–CO_2 inclusions (B-type FIs); (E) CO_2-dominated inclusions (C-type FIs) coexisting with B-type FIs, indicating immiscibility and CO_2 effervescence of the hydrothermal fluids.

3.2.2. B-type FIs

This FI type consists mainly of two phases, namely liquid water and a CO_2 vapor phase at room temperature (Fig. 4D). Occasionally, a liquid CO_2 phase is also observed. The FIs may be rounded or irregular in shape. The CO_2 phase occupies about 5–25% of the total volume of the FIs. The FIs developed along the same healed fractures usually have a constant volumetric proportion of CO_2. The relatively constant phase ratio is interpreted to have been resulted from the entrapment of a homogeneous fluid with no post-entrapment modification.

3.2.3. C-type FIs

The FIs contain one to two CO_2 phases (liquid and/or vapor) at room temperature (Fig. 4E). On slight heating (5 °C/min) from room temperature, the FIs usually homogenize to a vapor phase. Small amount of H_2O is occasionally observed to occur as a thin film rimming the inclusion walls or at the acute tips of inclusion walls.

3.3. Microthermometry

3.3.1. Homogenization temperature (T_h)

The observed homogenization temperatures (T_h) of FIs hosted in hydrothermal quartz of the Hetai goldfield are listed in Table 1 and displayed in Fig. 5. The temperatures range from 130 °C to 310 °C. There is no distinct difference in the T_h range between A- and B-type FIs. Statistically, the frequency distribution of T_h shows maxima at 245 °C and 170 °C (Fig. 5).

3.3.2. Final melting temperature of ice (T_m) and salinity

3.3.2.1. A-type FIs. The observed T_m ranges from −9.9 °C to −4.2 °C, and the calculated salinity varies from about 6 to 14 wt.% equiv. NaCl (Table 1). This indicates that the A-type FI type is moderately saline, compared to the B-type FIs.

3.3.2.2. B-type FIs. T_m ranges from about −3.4 °C to −0.9 °C, with the corresponding salinity of 2.7 to 5.6 wt.% NaCl equiv. (Table 1), indicating low salinities. The melting temperatures of CO_2 hydrate (T_{cm}) are 5.0 ± °C, corresponding to a salinity of about 2.1 wt.% NaCl equiv. Thus, the salinities of B-type FIs should be the maximum salinities (Lu et al., 2004).

In the T_h vs. salinity plot (Fig. 6), it is shown that A- and B-type FIs have similar range of T_h, but A-type FIs have higher salinities than those of B-type FIs.

3.3.3. First melting temperature (T_{fm})

The FIs change completely into a solid phase after being frozen to −120 °C. The first melting temperatures (T_{fm}) of the crystalline solids are measured during progressive heating.

3.3.3.1. A-type FIs. Many A-type FIs have T_{fms} of about −19.9 °C, indicating dominant NaCl (Table 1). Thus observation suggests that the classified moderate-salinity aqueous FIs are of a multicomponent system, with dominant H_2O–NaCl and the presence of Ca^{2+} (Roedder, 1984). The great variation of T_{fm} may be related to variation of the ratio of $CaCl_2$/NaCl in the ore-forming process.

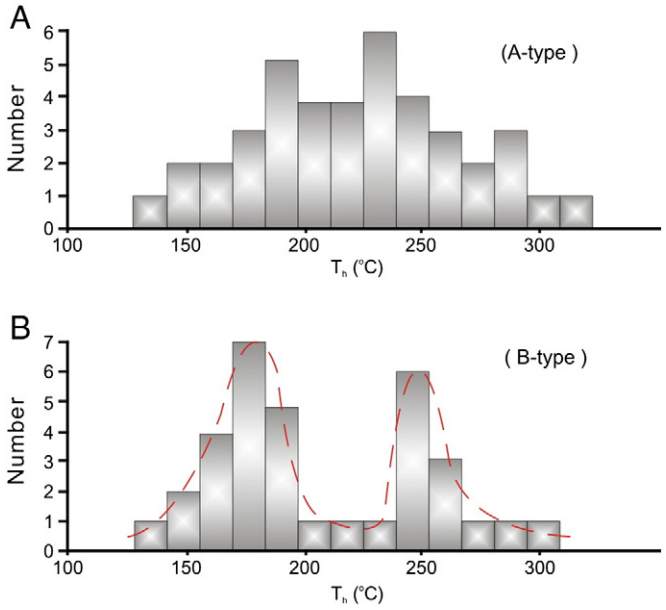

Fig. 5. Histogram for the observed homogenization temperatures (T_h) of FIs. (A) T_h of the A-type FIs; (B) T_h of the B-type FIs.

3.3.3.2. B-type FIs. Some FIs have initial melting temperatures of crystalline solids of −56.6 °C or below, and are characterized by the presence of a central vapor bubble of CO_2, plus minor amounts of other gaseous components (possibly CH_4 or H_2S). Therefore, we concluded that these inclusions are from a H_2O + NaCl + CO_2-dominant system.

3.3.3.3. C-type FIs. The first melting temperatures of this FI type range from −80 °C to −56 °C (Table 1), with a frequency maximum at around −56.6 °C, which is the eutectic temperature of the CO_2 system and therefore indicative of a CO_2-dominated system. A few FIs record a melting temperature lower than −56.6 °C, indicating the presence of a small amount of other gases such as H_2S and CH_4 in the inclusions.

3.3.4. Entrapment pressure

The trapping pressure of FIs may be estimated using the method described by Roedder (1984). The adopted procedure includes: (1) Based on the minimum and maximum densities, the range of isochors of A- and B-type FIs is defined on the P–T diagram using FLINCOR software (Brown and Lamb, 1989); and (2) the A- and B-type FIs with T_h ranging from 130 °C to 310 °C are selected to constrain the pressure. Using this method, the calculated pressure of FIs is 50–171 MPa for A-type FIs and 50–144 MPa for B-type FIs (Table 1).

4. Discussion

4.1. Characteristics and evolution of hydrothermal fluids

The ore-forming fluids from the Hetai deposit are characterized by mesothermal (mainly 170 °C–245 °C), CO_2-rich (e.g., B- and C-type FIs)

Table 1
Microthermometric data of fluid inclusions of the Hetai gold deposit.

Type of FIs	T_h (°C)	T_m (°C)	T_{cm} (°C)	T_{fm} (°C)	V% at 25 °C	Salinity (wt.% NaCl equiv.)	Bulk density (g/cm^3)	Pressure (MPa)
A	130–294	−9.9 to −4.2	ND	−20.8 to −19.9	10–25	6.7–13.9	0.84–1.02	50–171
B	130–310	−3.4 to −0.9	5.0	−61.2 to −56.6	10–20	2.7–5.6	0.70–0.96	50–144
C	ND	−8.6	13.7–30.2	−80.2 to −56.6	45–100	ND	ND	ND

Notation: T_h = homogenization temperature; T_m = final melting temperature of ice; T_{cm} = melt temperature of clathrate; T_{fm} = first melting temperature; V% at 25 °C = ratio of vapor phase at room temperature; wt.% NaCl equiv. = weight percent salt equivalent; bulk density and pressure were calculated using the FORTRAN program FLINCOR (Brown and Lamb, 1989); ND = not detected.

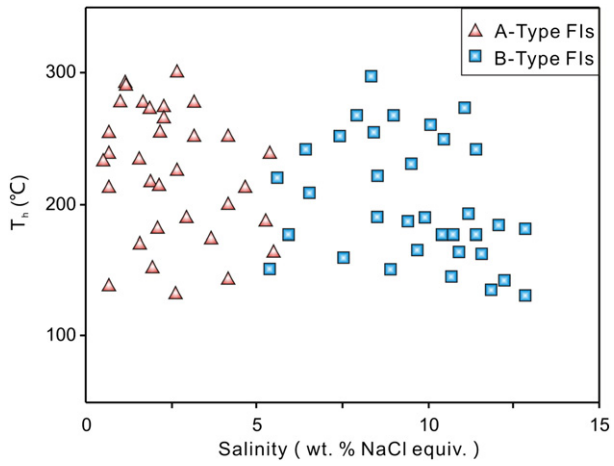

Fig. 6. Plot of homogenization temperature vs. salinity of the Hetai FIs. Two fields are well distinguished, i.e., the low salinity (A-type FIs) field marked with small rectangle and the moderate salinity (B-type FIs) field marked with small triangle.

and low salinities (below 10 wt.% NaCl equiv.), which is comparable to that found in many famous orogenic gold deposits in the world, such as those in the Yilgarn Craton and Bendigo goldfields in Australia (Hagemann and Luders, 2003; Thomas et al., 2011), the Donlin Creek gold deposit (Alaska) in North America (Goldfarb et al., 2004, 2013), the giant Sukhoi Log gold deposit (Siberia) in Russia (Large et al., 2007, 2009), as well as at Qinling and Jiaodong in China (Fan et al., 2003; Li et al., 2008, 2011; Nie, 1997; Zhou et al., 2002). In these gold deposits, moderately saline aqueous and CO_2-rich FIs are commonly present (Groves et al., 1998, 2003).

The fluid evolution of the Hetai goldfield is outlined in Fig. 7. The primary ore-forming fluid was a low salinity CO_2-bearing aqueous solution, which was initially a homogeneous supercritical phase located at the point a_1 above the solvus curve. During the ascent of the fluids, the temperature gradually dropped to a_2, resulting in the

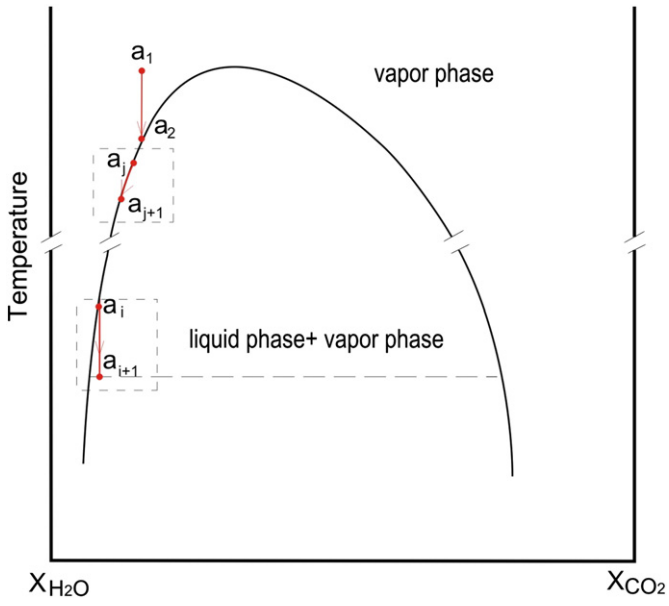

Fig. 7. The proposed hydrothermal fluid evolution path of the Hetai gold mineralization, and the topological composition–temperature phase diagram for H_2O–CO_2–NaCl system modified from Bowers and Helgeson (1983). Hydrothermal fluid evolution path from a_1 to a_2 is characterized by the entrapment of B-type FIs; CO_2 effervescence takes place along the path from a_j to a_{j+1}; unmixing of fluid occurs from a_i to a_{i+1}, accompanied by the formation of A- and C-type FIs.

deposition of hydrothermal quartz, sulfides, and captured B-type FIs (Fig. 4D). As the fluid evolution continued, CO_2 effervesced from the hydrothermal solution, following the path from a_j to a_{j+1}. At this point, fluid segregation took place (Fig. 4E). The primary hydrothermal fluid has segregated into two distinct phases, a more saline aqueous phase (presented by A-type FIs, Fig. 4C) and a CO_2-dominated phase (presented by C-type FIs, Fig. 4E), as fluid evolution progresses along the path from a_i to a_{i+1}. This segregation process may have alternated several times, and the dissolved solids became increasingly more saline. At Hetai, the coexistence of B- and C-type FIs in the same host grains provides direct evidence for this mechanism (Fig. 4 E). Judging from the bimodal distribution of T_h, at least two important segregation events may have taken place during the gold mineralization in the Hetai goldfield, i.e., the first occurred at 245 °C, and the second at 170 °C.

CO_2 effervescence and hydrothermal solution unmixing appear to have played an important role in gold deposition at Hetai. Experimental data and thermodynamic calculations demonstrate that a two-phase immiscibility domain for the H_2O–CO_2 system exists at low temperatures (Lu et al., 2004). The addition of NaCl into this system extends the two-phase domain to higher temperatures (Bowers and Helgeson, 1983). Recent literature has also revealed that for the proposed fluid evolution, immiscibility and CO_2 effervescence can lead to the formation of daughter mineral-bearing FIs, CO_2-dominated FIs and H_2O-dominated FIs (e.g., Zhang et al., 2012). Thus, a higher salinity aqueous fluid can be produced by the unmixing of a relatively low-salinity H_2O–CO_2 fluid.

4.2. Origin of ore-forming fluids

The mineralizing fluid preserved in the FIs of the Hetai goldfield is characterized by low salinity, low homogenization temperature and the presence of CO_2. This evidence, combining with geological, petrological and stable isotope data (Chen et al., 1988; Dai, 1986; Fu, 1988), can provide useful constraints on the possible sources of the mineralizing fluids.

Although granodiorite is widespread in the mining area, magmatic fluids cannot be the major source of the Hetai mineralizing fluids, because magmatic fluids are commonly highly saline brines trapped at higher temperature (400–700 °C) (Chen et al., 2007). Fluids derived from granitic magmas are generally characterized by $Na^+/K^+ < 1$ and $Cl^-/F^- < 1$ (Roedder, 1984), which are inconsistent with published inclusion leachate analyses and our microthermometry data of FIs which indicate that $Na^+ > K^+$ and $Cl^- > F^-$ (Table 1; Dai, 1986).

Therefore, the source(s) of the mineralizing fluids at Hetai may have been metamorphic or meteoric. It has been reported that CO_2-rich fluids are commonly found in high-grade metamorphic terrane regardless of host-rock composition (Chi et al., 2009; Jiang et al., 2009; Phillips et al., 1987). Another important characteristic of typical metamorphic fluids is a generally low salinity in calc-silicate rock area (Crawford, 1981). These characteristics are similar to those of the hydrothermal fluids at Hetai.

The O and H isotopes of the Au mineralization-related FIs at Hetai favor a metamorphic–meteoric fluid mixing hypothesis. The Hetai hydrothermal fluids fall in the transitional zone between the meteoric line and metamorphic fluid field, and far from the oceanic water field in the δD vs. $\delta^{18}O$ diagram (Chen et al., 1988; Fu, 1988). This indicates that meteoric water may have undergone O and H isotopic exchange between the metamorphosed country rocks and metamorphic fluids during circulation. This mixture may have evolved into the principal auriferous hydrothermal fluids, and subsequently migrated upward within the deformation zone.

4.3. Implications for ore genesis

The Hetai goldfield is located in the southern QHMB, which is interpreted as a tectonic suture that has experienced multiple

deformation due to terrane accretions from the Neoproterozoic to the Mesozoic (Shu et al., 2011; Zhao and Cawood, 2012; Zhou et al., 2012; Wang et al., 2013). The ore-forming age of the Hetai goldfield has been constrained by crosscutting relationships to be Indosinian (Triassic), as the gold-bearing mylonite zones are younger than the Shijian–Wuhe migmatite (378 to 263 Ma) but older than the Wucun monzonite (197 to 233 Ma) (Pirajno and Bagas, 2002; Wang et al., 1997).

The lodes are controlled by shear zones in the host rocks subjected to greenschist facies metamorphism (Fig. 2), and the gold grade is concentrated in shear zone centers regardless of the host rock lithologies. Native gold is the only major economic element, which is hosted in auriferous sulfide-bearing quartz veins.

The mesothermal ore-forming fluids are characterized by low salinity and high CO_2-rich, which may have originated from metamorphic fluids mixed with meteoric fluids (Chen et al., 2007; Phillips and Powell, 2010).

Based on the tectonic settings, ore deposit geology and FI study, we conclude that the Hetai goldfield is a typical orogenic gold deposit formed in the Indosinian Orogeny.

5. Conclusions

(1) The Hetai goldfield is evidently controlled by ductile shear zones in the greenschist facies metamorphosed host rocks.
(2) Three types of gold mineralization-related FIs have been newly identified, including the moderate-salinity aqueous (A-type), low-salinity H_2O–CO_2 (B-type) and CO_2-dominated (C-type) FIs.
(3) The low-salinity H_2O–CO_2 FIs may represent the primary mineralizing hydrothermal fluids, with CO_2 effervescence and unmixing occurring at about 245 °C and 170 °C, contributing to the gold precipitation.
(4) Ore forming fluids of the Hetai goldfield may have been originated from metamorphic fluids, a feature in accordance with typical orogenic gold deposits.

Acknowledgments

This study was financially supported by the China Geological Survey Project (No. 2010-01-15-33), the National Basic Research Program of China (2014CB440901) and NSFC Program (41402165, 41190073 and 41372198) and NSFC (41402165). Geological engineers of the No. 719 Geological Team and the Hetai Gold Corporation are thanked for their help during the field investigation. The recommendations and comments by Dr. Peter C. Lightfoot, Prof. F. Pirajno and two anonymous reviewers have greatly improved the paper. Cenozoic Geoscience Editing is acknowledged for its professional editing and language polishing service.

References

Bodnar, R.J., 1993. Revised equation and table for determining the freezing point depression of H_2O–NaCl solutions. Geochim. Cosmochim. Acta 57 (3), 683–684.
Bowers, T.S., Helgeson, H.C., 1983. Calculations of the thermodynamic consequences of nonideal mixing in the system H_2O–CO_2–NaCl on phase relations in geologic systems: metamorphic equilibria at high pressures and temperatures. Am. Mineral. 68, 1059–1075.
Brown, P.E., Lamb, W.M., 1989. P–V–T properties of fluids in the system $H_2O \pm CO_2 \pm$ NaCl: new graphic presentations and implications for fluid inclusion studies. Geochim. Cosmochim. Acta 53, 1209–1221.
Chen, Y.J., 2006. Orogenic type deposits and their metallogenic model and exploration potential. Geol. China 33, 1181–1196 (in Chinese with English abstract).
Chen, Y.J., Fu, S.G., 1992. Gold Mineralization in West Henan. Seismological Press, Beijing, pp. 1–234 (in Chinese with English abstract).
Chen, J., Wang, H., 1994. Distribution of REE and other trace elements in the Hetai gold deposit of South China: implications for evolution of an auriferous shear zone. J. Southeast Asian Earth Sci. 10, 217–226.
Chen, C.T., Ji, M.J., Hu, X.T., 1988. Preliminary analysis on the ore-forming conditions of the Hetai gold deposit, Guangdong. Geol. Guangdong 1, 1–16 (in Chinese with English abstract).
Chen, H.Y., Chen, Y.J., Liu, Y.L., 2001. Metallogenesis and its relationship with orogenesis of Erqs auriferous belt, Xinjiang. Sci. China D 44, 245–255 (in Chinese with English abstract).
Chen, Y.J., Ni, P., Fan, H.R., Lai, Y., 2007. Diagnostic fluid inclusions of different types gold deposits. Acta Petrol. Sin. 23, 2085–2108 (in Chinese with English abstract).
Chen, H.Y., Chen, Y.J., Baker, M.J., 2012a. Evolution of ore-forming fluids in the Sawayaerdun gold deposit in the Southwestern Chinese Tianshan metallogenic belt, Northwest China. J. Asian Earth Sci. 49, 131–144.
Chen, H.Y., Chen, Y.J., Baker, M.J., 2012b. Isotopic geochemistry of the Sawayaerdun orogenic-type gold deposit, Tianshan, northwest China: implications for ore genesis and mineral exploration. Chem. Geol. 310–311, 1–11.
Chi, G.X., Liu, Y., Dubé, B., 2009. Relationship between CO_2-dominated fluids, hydrothermal alterations and gold mineralization in the Red Lake greenstone belt, Canada. Appl. Geochem. 24 (4), 504–516.
Collins, P.L.F., 1979. Gas hydrates in CO_2-bearing fluid inclusions and use freezing data for estimation of salinity. Econ. Geol. 74, 1435–1444.
Crawford, M.L., 1981. Phase equilibria in aqueous fluid inclusions. Mineralogy Association of Canada Short Course Handbook. ,pp. 75–100.
Dai, T.G., 1986. Investigations on Metallogenetic Geochemistry of Hetai Gold Deposit, Western Guangdong ProvinceM.Sc Thesis Nanjing University, pp. 1–195, (in Chinese with English abstract).
Fan, H.R., Xie, Y.H., Zhai, M.G., Jin, C.W., 2003. A three stage fluid flow model for Xiaoqinling lode gold metallogenesis in the He'nan and Shanxi provinces, central China. Acta Petrol. Sin. 19, 260–266 (in Chinese with English abstract).
Fu, L.F., 1988. Some considerations on the relationship between the metamorphism of fractures and gold mineralization. Geol. Guangdong 1, 31–44 (in Chinese with English abstract).
Goldfarb, R.J., Groves, D.I., Cardoll, S., 2001. Orogenic Au and geologic time: a global synthesis. Ore Geol. Rev. 18, 1–75.
Goldfarb, R.J., Ayuso, R., Miller, M.L., Enert, S.W., Marah, E.E., Petsel, S.A., Miller, L.D., Bradly, D., Johnson, C., McClelland, W., 2004. The Late Cretaceous Donlin Creek Deposit, Southwestern Alaska: controls on epizonal formation. Econ. Geol. 99, 643–671.
Goldfarb, R.J., Taylor, R.D., Collions, G.S., Goryachev, N.A., Orlandini, O.F., 2013. Phanerozoic continental growth and gold metallogeny of Asia. Gondwana Res. http://dx.doi.org/10.1016/j.gr.2013.03.002.
Groves, D.I., Goldfarb, R.J., Gebre-Mariam, M., Hagemann, S.G., Robert, F., 1998. Orogenic gold deposits: a proposed classification in the context of their crustal distribution and relationship to other gold deposit types. Ore Geol. Rev. 13, 7–27.
Groves, D.I., Goldfarb, R.J., Robert, F., Hart, C.J.R., 2003. Gold deposits in metamorphic belts: overview of current understanding, outstanding problems, future research, and exploration significance. Econ. Geol. 98, 1–29.
Hagemann, S.G., Luders, V., 2003. P–T–X conditions of hydrothermal fluid and precipitation mechanism of stibnite–gold mineralization at the Wiluna lode-gold deposits, Western Australia: conventional and infrared microthermometric constraints. Miner. Deposita 38, 936–952.
Jiang, S.H., Nie, F.J., Hu, P., Lai, X.R., Liu, Y.F., 2009. Mayum: an orogenic gold deposit in Tibet, China. Ore Geol. Rev. 36, 160–173.
Kerrich, R., Goldfarb, R.J., Groves, D.I., Garwin, S., Jia, Y.F., 2000. The characteristics, origins and geodynamic setting of supergiant gold metallogenic provinces. Sci. China D 43, 1–68 (supp.).
Large, R., Maslennikov, V., Robert, F., 2007. Multistage sedimentary and metamorphic origin of pyrite and gold in the giant Sukhoi Log, Lena gold province, Russia. Econ. Geol. 102, 1233–1267.
Large, R., Danyushevsky, L., Hollit, C., Maslennikov, V., Meffre, S., Gilbert, S., Bull, S., Scott, R., Emsbo, P., Thomas, H., Singh, B., Foster, J., 2009. Gold and trace element zonation in pyrite using a laser imaging technique: implications for the timing of gold in orogenic and carlin-style sediment-hosted deposits. Econ. Geol. 104, 635–668.
Li, Z.L., Zhai, W., Huang, D.L., Zhao, W.X., Yang, R.Y., Quan, Y.R., Li, W., 2001. The discovery of melt inclusions in Hetai and Qiaogashan ductile shear zone gold deposits and genetic study of these deposits. Miner. Deposita 20, 208–215 (in Chinese with English abstract).
Li, N., Sun, Y.L., Li, J., Xue, L.W., Li, W.B., 2008. The molybdenite Re–Os isotope age of the Dahu Au–Mo deposit, Xiaoqinling and the Indosinian mineralization. Acta Petrol. Sin. 24, 810–816 (in Chinese with English abstract).
Li, N., Chen, Y.J., Fletcher, R., Zeng, Q.T., 2011. Triassic mineralization with Cretaceous overprint in the Dahu Au–Mo deposit, Xiaoqinling gold province: constraints from SHRIMP monazite U–Th–Pb geochronology. Gondwana Res. http://dx.doi.org/10.1016/j.gr.2010.12.013.
Li, J.W., Bi, S.J., Selby, D., Chen, L., Vasconcelos, P., Thiede, D., Zhou, M.F., Zhao, X.F., Li, Z.K., Qiu, H.N., 2012. Giant Mesozoic gold provinces related to the destruction of the North China Craton. Earth Planet. Sci. Lett. 349–350, 26–37.
Liu, W., Huang, M.X., Ouyang, Y.F., 2005. Characteristics of mineralization fluids in the Hetai gold deposit of Guangdong. Mineral Resour. Geol. 19, 469–474 (in Chinese with English abstract).
Lu, H.Z., Fan, H.R., Ni, P., Ou, X.G., Shen, K., Zhang, W.H., 2004. Fluid Inclusion. Science Press, Beijing, pp. 1–487 (in Chinese with English abstract).
Nie, F.J., 1997. An overview of the gold resources of China. Int. Geol. Rev. 39, 55–81.
No.719 Geological Team, 1987. Report of Geological Prospecting for the Gaocun Ore Deposit in the Hetai Gold Field. ,pp. 1–185, (in Chinese).
Phillips, G.N., Powell, R., 2010. Formation of gold deposits: a metamorphic devolatilization model. J. Metamorph. Geol. 28 (6), 689–718.
Phillips, G.N., Groves, D.I., Brown, I.J., 1987. Source requirements for the Golden Mile, Kalgoorlie: significance to the metamorphic replacement model for Archean gold deposits. Can. J. Earth Sci. 24, 1643–1651.
Pirajno, F., 2009. Hydrothermal Processes and Mineral System. Springer, Berlin, pp. 1–1250.

Pirajno, F., Bagas, L., 2002. Gold and silver metallogeny of the South China Fold Belt: a consequence of multiple mineralizing events? Ore Geol. Rev. 20, 109–126.
Reich, M., Kesler, S.E., Utsunomiya, S., Palenik, C.S., Chryssoulis, S.L., Ewing, R., 2005. Solubility of gold in arsenian pyrite. Geochim. Cosmochim. Acta 69, 2781–2796.
Roedder, E., 1984. Fluid Inclusions: Reviews of Mineralogy. ,pp. 1–644.
Shu, L.S., Faure, M., Yu, J.H., Jahn, B.M., 2011. Geochronological and geochemical features of the Cathaysia block (South China): new evidence for the Neoproterozoic breakup of Rodinia. Precambrian Res. 187 (3–4), 263–276.
Thomas, H., Large, R., Bull, S.W., Maslennikov, V., Berry, R.F., Fraser, R., Froud, S., Moye, R., 2011. Pyrite and pyrrhotite texture and composition in sediments, laminated quartz veins, and reefs at Bendigo Gold Mine, Australia: insight for ore genesis. Econ. Geol. 106, 1–31.
Wang, S.L., Yao, X., 2001. The experiences in resource utilization and approaches to prospecting foe reserves increase in Hetai gold mine. Gold Sci. Technol. 9, 44–52 (in Chinese with English abstract).
Wang, H.N., Chen, J., Ji, J.F., Qu, X.M., 1997. Geological and geochemical characteristics of the Hetai gold deposit, South China: gold mineralization in an auriferous shear zone. Int. Geol. Rev. 39, 181–190.
Wang, Y.J., Fan, W.M., Guo, F., Peng, T.P., 2003. Geochemistry of Mesozoic mafic rocks around the Chenzhou–Linwu fault in South China: implication for the lithospheric boundary between the Yangtze and the Cathaysia Blocks. Int. Geol. Rev. 45 (3), 263–286.
Wang, Y.J., Fan, W.M., Cawood, P.A., Li, S.Z., 2008. Sr–Nd–Pb isotopic constraints on multiple mantle domains for Mesozoic mafic rocks beneath the South China Block hinterland. Lithos 106, 297–308.
Wang, Y.J., Fan, W.M., Zhang, G.W., Zhang, Y.H., 2013. Phanerozoic tectonics of the South China Block: key observations and controversies. Gondwana Res. http://dx.doi.org/10.1016/j.gr.2012.02.019.
Zhang, G., Boulter, C.A., Liang, J., 2001. Brittle origins for disseminated gold mineralization in mylonite: Gaocun gold deposit, Hetai goldfield, Guangdong Province, South China. Econ. Geol. 96, 49–59.
Zhang, L., Zheng, Y., Chen, Y.J., 2012. Ore geology and fluid inclusion geochemistry of the Tiemurt Pb–Zn–Cu deposit, Altay, Xinjiang, China: a case study of orogenic-type Pb–Zn systems. J. Asian Earth Sci. 49, 69–79.
Zhang, J., Deng, J., Chen, H.Y., Yang, L.Q., Cooke, D., Danyushevsky, L., Gong, Q.J., 2014. LA-ICP-MS trace element analysis of pyrite from the Chang'an gold deposit, Sanjiang region, China: implication for ore-forming process. Gondwana Res. 26, 557–575.
Zhao, G., Cawood, P.A., 2012. Precambrian geology of China. Precambrian Res. 222–223, 13–54.
Zhou, Y.Z., 1992. Geochemistry and Metallogenetic Mechanism of the Hetai Goldfield, South ChinaDoctoral Thesis of Quebec University ,pp. 1–279.
Zhou, Y.Z., Chown, E.H., Guha, J., Lu, H.Z., Tu, G.Z., 1994a. Hydrothermal origin of Precambrian bedded chert at Gusui, Guangdong, China: petrologic and geochemical evidence. Sedimentology 3, 605–619.
Zhou, Y.Z., Tu, G.Z., Chown, E.H., Guha, J., Lu, H.Z., 1994b. Ductile deformation, hydrothermal alteration and associated geochemical behaviors of trace elements in Hetai gold field, Guangdong, China. Comparative Study of Gold Deposits in Canada and China, Beijing. Seismic Press, pp. 63–77 (in Chinese with English abstract).
Zhou, Y.Z., Chown, E.H., Tu, G.Z., 1995. Petrologic and geochemical study of metamorphic Upper Precambrian strata in Shidong–Wuhe–Shijiang–Hetai district of Guangdong Province, China. Acta Geol. Sin. 1, 33–52 (in Chinese with English abstract).
Zhou, T., Goldfarb, R.J., Phillips, G.N., 2002. Tectonics and distribution of gold deposits in China—an overview. Miner. Deposita 37, 249–282.
Zhou, Y.Z., Zeng, C.Y., Li, H.Z., An, Y.F., Lu, W.C., Yang, Z.J., Shen, W.J., 2012. Geological evolution and ore-prospecting targets in southern segment of Qinzhou-Bay–Hangzhou Bay juncture orogenic belt, southern China. Geol. Bull. China 31, 486–491 (in Chinese with English abstract).